Metalurgi (2024) 3: 107-116

METALURGI
Majalah Ilmu dan Teknologi
p-ISSN 0126-3188 | e-ISSN 2443-3926
ejurnalmaterialmetalurgi.lipi.go.id

SELF-HEALING BEHAVIOR OF HYDROTHERMALLY ENGINEERED HAP/PAA COATINGS ON MAGNESIUM ALLOY WE43

Aprilia Erryani[a, b, *], Fendy Rokhmanto[a, b], Albertus Deny Heri Setyawan[b], Yudi Nugraha Thaha[b], Ahmad Zakiyuddin[a], Ika Kartika[b], Sri Harjanto[a,*]

[a]Department of Metallurgical and Materials Engineering, University of Indonesia
Kampus UI, Kukusan, Depok, Indonesia 16424
[b]Research Center for Metallurgy, National Research and Innovation Agency (BRIN)
B.J. Habibie Sains and Technology Area, Banten, Indonesia 15314
*E-mail: aprilia.erryani@gmail.com; sri.harjanto@ui.ac.id

Received: 23-10-2025, Revised: 16-12-2025, Accepted: 17-12-2025

Abstract

This work examines the self-healing properties and corrosion prevention mechanisms of hydrothermally synthesized HAp/PAA (hydroxyapatite/polyacrylic acid) composite coatings on magnesium alloy WE43. The coatings were produced with different PAA concentrations (0.15, 0.3, and 0.5 wt.%) by a hydrothermal method at 140 °C for 3 hours. The composite layers were analyzed using FTIR (fourier transform infrared spectroscopy), SEM (scanning electron microscopy), and EIS (electrochemical impedance spectroscopy) to assess their structural and electrochemical properties, as well as their self-healing capabilities via a scratch–immersion test in Hank's solution at 37 °C for 48 hours. FTIR analysis confirmed the simultaneous presence of HAp and PAA phases without any chemical reaction, indicating physical contact through hydrogen bonding. The elevation of PAA concentration markedly affected coating morphology, resulting in denser and more uniform structures characterized by spherical HAp crystals at 0.5 wt.% PAA. SEM analysis following scratching and immersion demonstrated that the 0.5 wt.% PAA coating successfully preserved surface integrity and displayed partial restoration of the injured region via the reprecipitation of Ca–P compounds. The EIS findings indicated that the 0.5 wt.% PAA coating maintained the maximum impedance modulus (>10^4 Ω·cm²) and a steady phase angle after 48 hours of immersion, therefore affirming its exceptional corrosion resistance and self-healing properties. The results demonstrate that an ideal PAA content fosters a dense, ion-responsive hybrid layer that effectively reinstates barrier characteristics following mechanical impairment. The hydrothermally produced 0.5 wt.% HAp/PAA coating offers an efficient self-healing and corrosion-resistant surface for WE43 magnesium alloy, indicating significant potential for use in next-generation biodegradable implant systems.

Keywords: *Magnesium WE43, hydroxyapatite, polyacrilic acid, hydrothermal coating, self-healing*

1. INTRODUCTION

The concept of self-healing coating has recently gained significant attention in the advancement of biodegradable implant materials. This coating can autonomously restore its protective function following damage, thus prolonging the material's service life and mitigating localized corrosion [1]-[2]. Self-healing mechanisms are crucial for magnesium (Mg)-based materials and their alloys, which, despite exhibiting biocompatibility and mechanical properties similar to natural bone, encounter the challenge of rapid degradation in physiological environments. The elevated corrosion rate results in hydrogen gas production, a rise in local pH, and a reduction in mechanical strength before the complete regeneration of bone tissue [3].

Magnesium alloy WE43 is recognized for its high strength and favorable biocompatibility, attributed to its composition of yttrium (Y), rare earth (RE), and zirconium (Zr) elements [4]-[5].

DOI: 10.55981/metalurgi.2024.780

Metalurgi is Sinta 2 Journal (https://sinta.kemdikbud.go.id/journals/profile/3708) accredited by Ministry of Education, Culture, Research, and Technology, Republic Indonesia

The increased corrosion rate in the body's environment continues to be a significant limitation [6]. A surface system is required that offers protection against corrosion and possesses the ability to self-heal following mechanical or chemical damage [7].

A prevalent method involves the application of hydroxyapatite (HAp) due to its chemical resemblance to bone minerals and its osteoconductive properties[8]-[9]. Pure HAp layers exhibit brittleness, susceptibility to cracking, and weak adhesion to magnesium substrates. Various studies have addressed these weaknesses by combining HAp with biocompatible polymers to enhance the flexibility and interfacial strength of the layers[10]-[11].

PAA is a promising hydrophilic polymer distinguished by a high density of carboxylate groups (-COOH) [12]. These groups bind to calcium ions and form hydrogen bonds with phosphate groups from HAp, which improves adhesion and makes the layers more uniform [13]. PAA acts as an ionic reservoir and diffusion regulator, helping the protective layer to rebuild in places where it has been damaged [14]. The soaking procedure in physiological solution lets the PAA phase move Ca^{2+} and PO_4^{3-} ions to the scratched sites, which helps build protective compounds like HAp or Ca–P crystals. This process creates a self-healing mechanism that rebuilds the protective layer, sealing up microcracks and restoring the barrier's ability to guard against corrosion [15]-[16].

This phenomenon is increasingly reported; however, the systematic study of the relationship between PAA concentration, layer morphology, and self-healing efficiency remains limited. The level of self-healing ability is significantly affected by the microstructure of the layer, ion mobility, and the organic-inorganic ratio in the composite, all of which can be regulated through hydrothermal synthesis parameters.

This study synthesized HAp/PAA composite layers on magnesium alloy WE43 via the hydrothermal method, utilizing varying PAA concentrations of 0.15%, 0.3%, and 0.5% w/v. This study examined the impact of PAA content on self-healing properties and the mechanisms underlying corrosion protection following mechanical surface damage. Evaluation was performed through scratch-immersion testing in Hank's solution and EIS (electrochemical impedance spectroscopy) analysis to assess the evolution of coating integrity over immersion time. This research aims to enhance understanding of the dynamic self-healing mechanism in the HAp/PAA composite system and its potential application as an adaptive smart coating for next-generation biodegradable magnesium implants.

2. MATERIALS AND METHODS

The research employed commercial magnesium alloy WE43, acquired from Smith Metal Products Co., Ltd., UK. The alloys contain 3.7-4.3% Y, 2.4-4.4% RE (Nd, Gd), and 0.4% Zr by weight. The specimens were subjected to wet abrasion with SiC paper up to a 3000-grit level, utilizing ethanol spray as a lubricant. Subsequently, polishing was conducted with a micro cloth utilizing diamond paste of varying particle sizes: 8, 6, 3, 1, and 0.1 μm, respectively. The object underwent ultrasonic cleaning in ethanol for 10 minutes, followed by air drying at ambient temperature. The compounds listed are $Ca(NO_3)_2{\cdot}4H_2O$ and $Na_2HPO_4{\cdot}2H_2O$, both with a purity of 99.9% from Merck. PAA possesses a molecular weight ranging from 800 to 1000 gr/mol. The PAA-HAp coating was applied using the hydrothermal method within a 75 mL reaction autoclave containing a Ca-P solution. A hydrothermal solution was prepared by dissolving 0.05 M calcium nitrate tetrahydrate ($Ca(NO_3)_2{\cdot}4H_2O$) and 0.03 M sodium phosphate dibasic dihydrate ($Na_2HPO_4{\cdot}2H_2O$). The properties of the polymer were analyzed by varying the composition to include 0.15, 0.3, and 0.5 w/v% of PAA in deionized water. Subsequently, the magnesium alloy WE43 was immersed in the deposition solution, positioned within the autoclave, and subjected to heating in an electric oven at a temperature of 140°C. Following a period of 3 hours, the PAA-HAp/Mg samples were subjected to multiple rinses with deionized water and 95% ethanol. Subsequently, a drying process was conducted at a temperature of 60°C to eliminate any impurities.

The coatings' functional groups were analyzed using an FTIR (fourier-transform infrared spectrophotometer) with ATR (attenuated total reflectance) Bruker Alpha II. The coatings' surface morphology and elemental composition were analyzed using a scanning electron microscope (SEM; JEOL JSM-6390). The self-healing capability of the coatings was examined through the scratching method, while the corrosion behavior of the samples was analyzed using electrochemical impedance spectroscopy. A straight scratch was introduced on the coating surface using a stainless-steel blade with a hemispherical tip (tip radius ~20–30 μm) under a constant normal load of 2 N, in accordance with the manual scratch procedures described in ISO 1518-1 and ASTM C1624. The scratch length was approximately 5–8 mm with a controlled

scratching speed of ~1 mm·s^{-1}. The sample was subsequently immersed in Hank's solution at 37°C for a duration of up to 48 hours. The self-healing capability was assessed at 24-hour and 48-hour immersion intervals. Electrochemical impedance spectroscopy (EIS) was conducted using an AutoLab 302 Multi BA electrochemical workstation with Hank's solution (pH 7.4–7.2) at a temperature of 37±1 °C. A three-electrode electrochemical configuration was utilized, comprising a coated WE43 specimen as the working electrode, an Ag/AgCl reference electrode saturated in KCl, and a platinum counter electrode for the electrochemical assessment. The samples were permitted to stabilize at their open circuit potential (OCP) for 5 minutes before the commencement of measurements.

3. Results and Discussion

3.1 Chemical Composition

Figure 1 shows the FTIR spectra of the autoclaving-synthesized HAp/PAA composite coatings on WE43 magnesium alloy with varying PAA concentrations (0.15, 0.3, and 0.5 weight %). The O–H stretching vibrations are related to a broad absorption band observed about 3400 cm^{-1}, which indicates that there are hydroxyl groups from HAp and maybe some water that has been absorbed. Characteristic peaks at around 1700 cm^{-1} have been assigned to the stretching vibrations of carbonyl (C=O) groups from PAA. Clearly visible C–H stretching vibrations about 2900 cm^{-1} confirm the inclusion of the organic PAA phase within the coatings.

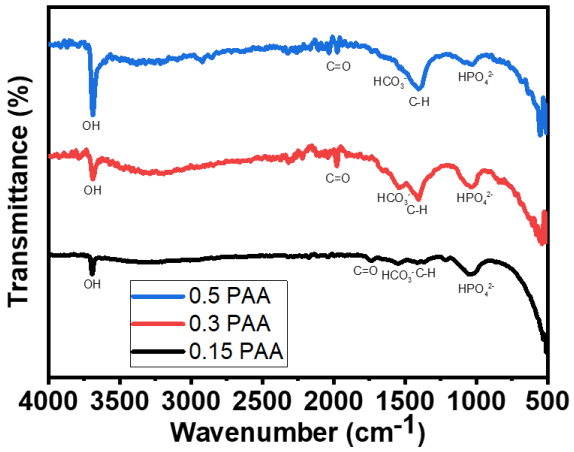

Figure 1. FTIR spectra of magnesium WE 43 coated hydrothermally HAp with a varying composition of PAA

In addition, assigned to the phosphate (HPO_4^{2-}) groups of HAp are significant absorption bands between 1000 and 1100 cm^{-1}, therefore showing the effective development of the inorganic HAp phase. Higher PAA concentrations were shown to cause an increase in the intensity of the C=O and C–H peaks, therefore suggesting a larger polymeric phase contribution in the composite coating. On the other hand, the quite constant phosphate-related peaks indicate that the HAp level was kept constant throughout all the samples. These findings demonstrate that the HAp/PAA composite coatings were effectively generated without any notable chemical reactions and that the connection between HAp and PAA is most likely physical and involves hydrogen bonding [17].

3.2 Surface Morphology

Figure 2 presents the surface morphologies of the hydrothermally synthesized HAp/PAA composite coatings on magnesium alloy WE43 with varying PAA concentrations of (a) 0.15%, (b) 0.3%, and (c) 0.5% (w/v). The variation in PAA concentration markedly affects the nucleation behavior, particle dispersion, and compactness of the coating layers.

At the lowest PAA concentration (0.15%, Fig. 2(a)), the surface shows an inhomogeneous and coarse morphology, characterized by large agglomerated HAp clusters and noticeable voids between them. The uneven distribution of particles indicates insufficient stabilization of HAp precursors, resulting in uncontrolled crystal growth and a porous coating structure. Such morphology may lead to reduced barrier properties and increased susceptibility to corrosion.

When the PAA concentration increases to 0.3% (Fig. 2(b)), the coating surface becomes denser and more uniform, with smaller and more evenly distributed particles. The presence of an adequate amount of PAA improves dispersibility and controls the nucleation of HAp, forming a relatively compact and continuous layer [18]. However, minor textural irregularities are still visible, suggesting partial agglomeration during growth. At the highest concentration (0.5% PAA, Fig. 2(c)), the surface morphology transforms into a fine, compact layer composed of uniformly distributed spherical-like HAp crystals. The excess PAA promotes rapid nucleation while restricting further crystal growth, producing nanosized spherical particles that tightly fill the surface. This morphology results in a smooth and highly compact coating, indicating improved interface coverage and reduced surface defects. The uniform and dense arrangement of spherical HAp particles likely enhances corrosion protection by limiting electrolyte penetration and stabilizing the interfacial layer [19]. 3.3 Self-Healing Evaluation

Figure 3 shows how the scratched HAp/PAA coatings on the WE43 alloy looked before and

after being put in Hank's solution for 24 and 48 hours. The changes in surface characteristics can tell us about how well each coating composition can repair itself, how well it stays intact, and how it reacts to corrosion. In the first stage (Figs. 3(a), 3(d), and 3(g)), the scratched regions are easy to see on all of the coatings. This sign indicates that mechanical damage has exposed the substrate. The surface of the 0.15 PAA coating (Fig. 3(a)) is very rough, and debris builds up unevenly along the scratch. The 0.3 PAA (Figure 3d) and 0.5 PAA (Fig. 3(g)) coatings, on the other hand, seem more compact and continuous, which means they stick better and are stronger. The 0.5 PAA sample, in particular, has a smoother and denser surface surrounding the scratch. This suggests that the composite layer and the substrate are more strongly bonded at the interface [20].

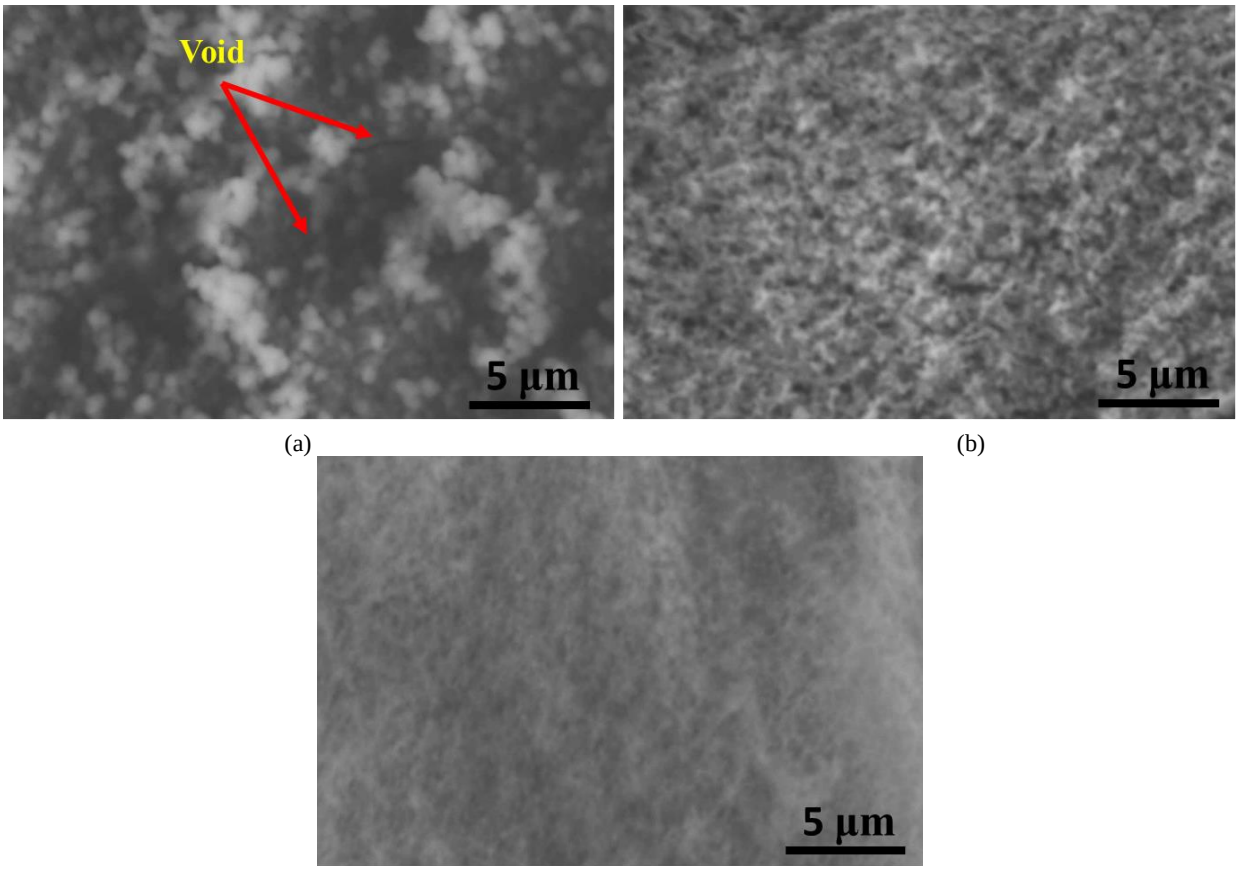

(a) (b)

(c)

Figure 2. SEM image of magnesium WE 43 coated HAp with PAA (a) 0.15 PAA, (b) 0.3 PAA, and (c) 0.5 PAA (w/v)

When a scratch occurs, the electrolyte gets into the coating and penetrates the green layer and magnesium substrate below, which starts localized corrosion. This makes $Mg(OH)_2$ and raises the pH in the area that was impacted. The alkaline environment speeds up the precipitation of phosphate and allows the coating and immersion medium absorb Ca^{2+} ions. This leads to the formation and growth of calcium phosphate phases. These deposits slowly turn into hydroxyapatite (HAp), which fills in and seals the scratched region. The created layer effectively blocks aggressive ion movement and stops more electrolyte from getting in, which reduces localized corrosion and makes self-healing capabilities easier to achieve [21]-[22].

After 24 hours of immersion (Figs. 3(b), 3(e), and 3(h)), the coatings show clear differences. The 0.15 PAA sample (Fig. 3(b)) displays clear microcracks and localized corrosion products developing along the scratch lines. This suggests that the coating wasn't able to keep the electrolyte from getting through. The 0.3 PAA coating (Fig. 3(e)) produces a denser network of microcracks, although the surface is still mostly intact. The 0.5 PAA coating (Fig. 3(h)), on the other hand, is mostly intact, showing only minor surface fractures and an absence of major pitting. This implies that the increased concentration of PAA made the coating more compact and less susceptible to damage in specific areas. After 48 hours of immersion (Figs. 3(c), 3(f), and 3(i)), the lower-PAA coatings show greater signs of deterioration. The 0.15 PAA sample (Fig. 3(c)) shows a lot of delamination and deep fissures, which means that the magnesium substrate

underneath is corroding a lot. The 0.3 PAA coating (Fig. 3(f)) is partially coming off and collecting corrosion products, which means it offers modest protection. The 0.5 PAA coating (Fig. 3(i)), on the other hand, keeps a smooth and continuous surface with only a few signs of corrosion. The fine, round HAp crystals and increased polymer content probably made the microstructure more compact, which stopped ions from moving around and protected the substrate while it was in hanks'solution for a long time [23].

Overall, the microstructural evolution during immersion demonstrates that increasing PAA concentration improves the coating's ability to withstand corrosion and maintain surface integrity after mechanical damage. Among the tested compositions, the coating prepared with 0.5% PAA exhibits the best corrosion resistance and healing behavior, characterized by minimal crack propagation and the presence of a stable protective layer after 48 h of immersion [24]

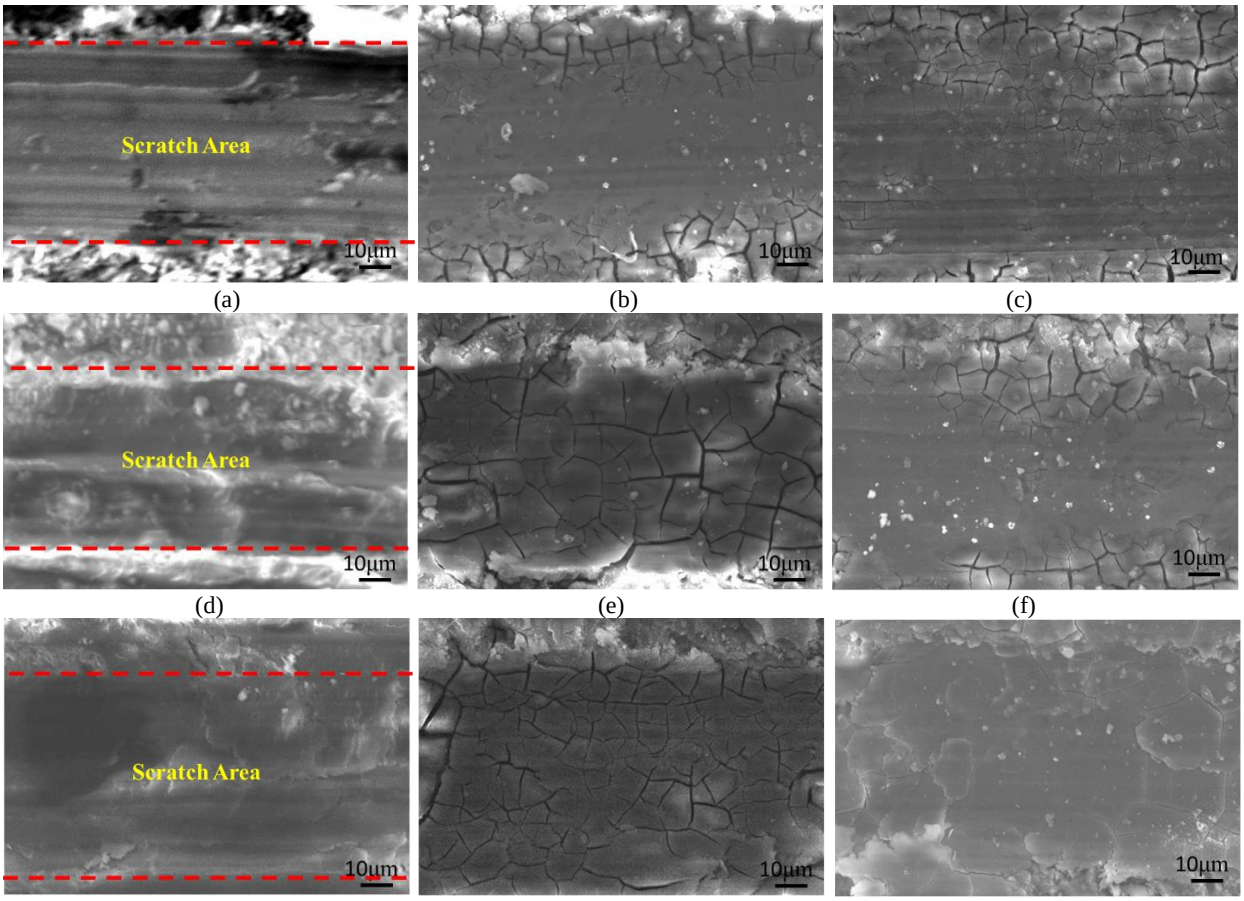

Figure 3. SEM image of the coating's surface morphology in the scratch-immersion test on the HAp/PAA-coated WE43 alloy: (a) 0.15 PAA just after scratching, (b) 0.15 PAA after 24 h, and (c) 0.15 PAA after 48 h, (d) 0.3 PAA just after scratching, (e) 0.3 PAA after 24 h, and (f) 0.3 PAA after 48 h, (g) 0.5 PAA just after scratching, (h) 0.5 PAA after 24 h, and (i) 0.5 PAA after 48 h of immersion in Hanks' solution at 37 °C

Figure 4 shows the electrochemical impedance spectra of the HAp/PAA coatings on WE43 alloy with varied PAA concentrations (0.15%, 0.3%, and 0.5% w/v). The spectra were taken at different periods of immersion (before scratching, after scratching, and after 24 and 48 hours of immersion in Hank's solution). The Nyquist plots (Figs. 4(a), 4(d), and 4(g)), Bode modulus plots (Figs 4(b), 4(e), and 4(h)), and Bode phase plots (Figs 4(c), 4(f), and 4(i)) show how the coating's electrochemical response and protective stability change over time while it is in Hank's solution.

For the coating with 0.15% PAA (Figs 4(a)-4(c)), the Nyquist diagram displays a small capacitive semicircle with a noticeable reduction in diameter after scratching and immersion. The impedance modulus at low frequencies ($|Z|_{0.01Hz}$) decreases sharply after 24 h, indicating the rapid loss of protective properties. The Bode phase plot shows a single relaxation time that shifts toward lower frequencies, confirming that corrosion processes dominate after electrolyte penetration. These results are consistent with the SEM observations (Figs. 3(a)-3(c)), where extensive cracking and delamination occurred, suggesting that the porous and inhomogeneous coating formed at low PAA concentration provides insufficient corrosion protection [25].

For 0.3% PAA (Figs. 4(d)-4(f)), the Nyquist plots show bigger capacitive loops and higher impedance values than for 0.15% PAA. This means that the barrier works better. The Bode phase diagram shows two-time constants, one for the outside porous HAp/PAA layer and one for the inner corrosion product layer. After 48 hours of immersion, though, there is a slight drop in impedance, which suggests that the coating is breaking down in some way. The electrochemical trends are in line with the SEM results (Figs. 3(d)-3(f)), which reveal that the 0.3% PAA coating keeps its structure better than the 0.15% PAA coating but develops microcracks and localized corrosion characteristics with time.

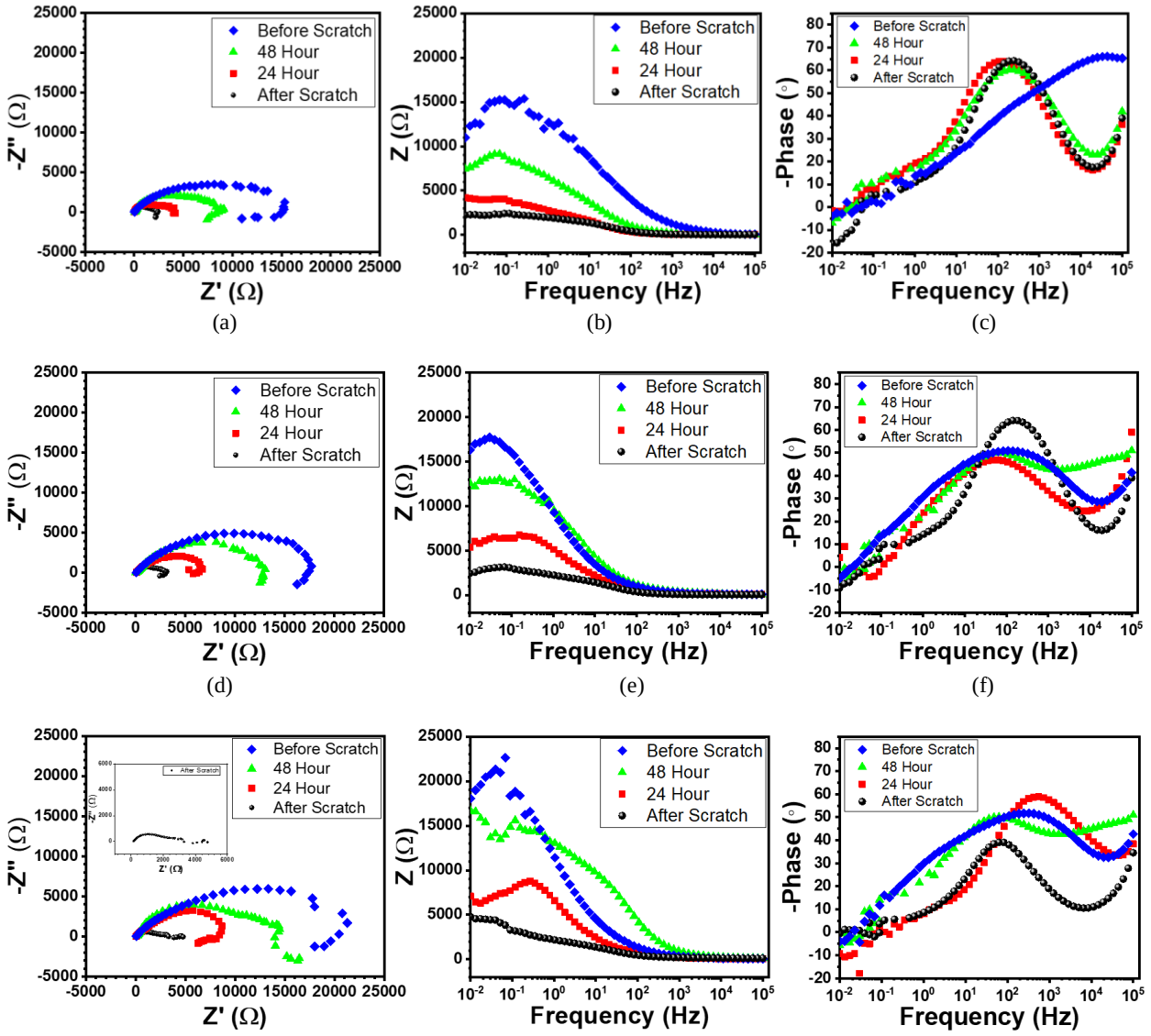

Figure 4. Electrochemical impedance spectra of the scratch-immersion test on the HAp/PAA-coated WE43 alloy: (a) Nyquist plot of 0.15 PAA, (b) Bode Modulus plot of 0.15 PAA (c) Bode Phase plot of 0.15 PAA, (d) Nyquist plot of 0.3 PAA, (e) Bode Modulus plot of 0.3 PAA (f) Bode Phase plot of 0.3 PAA, (g) Nyquist plot of 0.5 PAA, (h) Bode Modulus plot of 0.5 PAA (i) Bode Phase plot of 0.5 PAA

The coating with 0.5% PAA (Figs. 4(g)-4(i)) demonstrates the highest impedance values and the largest Nyquist semicircle radius, even after 48 h of immersion. The Bode modulus remains above 10^4 Ω·cm² at low frequencies, and the phase angle approaches −70°, indicating a highly capacitive and protective surface. The two distinct time constants persist, suggesting stable dual-layer protection consisting of a compact outer HAp/PAA layer and a corrosion-resistant interface layer beneath it. Only a minor reduction in impedance is observed after scratching, demonstrating that the coating effectively limits electrolyte access and exhibits partial self-healing capability. These findings are consistent with SEM observations (Figs. 3(g)-3(i)), where the 0.5% PAA coating retained a smooth, dense morphology with minimal cracking after

prolonged immersion. The presence of spherical and uniformly distributed HAp crystals, as seen in Fig. 2(c), contributes to the formation of a tightly packed microstructure that enhances barrier resistance and adhesion [26].

In general, the EIS results back up what the SEM investigations found about how the shapes changed. The corrosion resistance and coating stability of the HAp/PAA composite layers become a lot better when the PAA concentration Figure 5 presents equivalent circuits calculated from the Nyquist plot characterization results of the scratch-immersion test. The variations in the equivalent circuit models derived from each PAA composition and immersion condition illustrate the dynamic and intricate characteristics of the HAp/PAA composite layer system throughout the degradation process. The model's inconsistency or randomness arises not from measurement errors, but from actual alterations in the structure of the metal layers and interfaces during the scratch-immersion test. In the layer with low PAA content (0.15%), the porous structure yields a straightforward electrochemical response characterized by one to two time constants. In contrast, at 0.3% PAA, the system exhibits goes up. The 0.5% PAA coating has the most stable electrochemical behavior of all the formulations. Even after mechanical damage or prolonged immersion in water, it maintains high impedance values and phase stability. The compact, spherical HAp shape and the thick PAA polymer matrix work together to stop corrosion reactions and keep the metal-coating contact stable, which is why the formulation works so well [27].

increased complexity due to the development of a double protective layer and regenerative reactions in the scratched region. At 0.5% PAA, the thicker and more hydrophilic layer is capable of absorbing water, which facilitates the formation of ionic diffusion pathways and results in an inductive response at low frequencies. This difference shows that the protective mechanisms in each case are not static; they change over time and are affected by the layer's organic-inorganic composition. The variety of equivalent circuit models reinforces the understanding that corrosion and film recovery processes occur progressively and adaptively in response to environmental conditions.

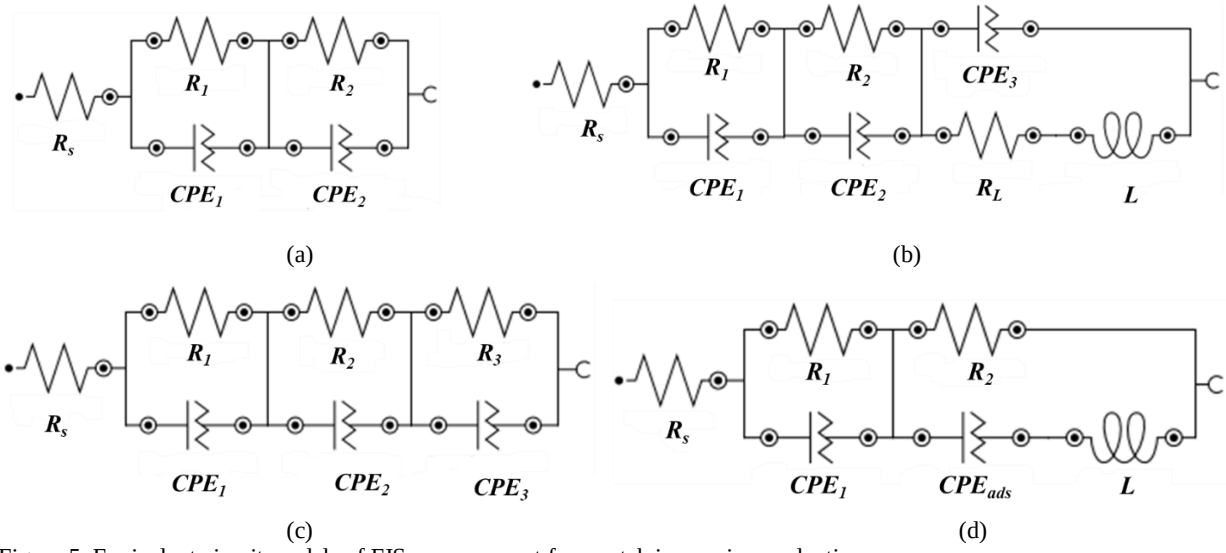

Figure 5. Equivalent circuit models of EIS measurement for scratch immersion evaluation

4. CONCLUSION

The hydrothermally synthesized hydroxyapatite/polyacrylic acid (HAp/PAA) composite coating was proven to enhance corrosion resistance and exhibit effective self-healing behavior on WE43 magnesium alloy. Variations in PAA concentration play a crucial role in determining the microstructure, density, and stability of the layer. The increased PAA content results in better dispersion of HAp crystals and promotes the formation of a dense and homogeneous microstructure, thereby strengthening the interface between the layers and the substrate. FTIR analysis indicates that HAp and PAA physically interact through hydrogen bonds without forming new compounds, while SEM results show that the layer with 0.5% PAA can maintain its surface integrity even after mechanical damage. During the soaking process in Hank's solution, the PAA phase acts as an ionic reservoir, facilitating the migration of Ca^{2+} and PO_4^{3-} ions toward the

scratched areas, thus leading to the re-formation of Ca–P compounds or HAp crystals that seal microcracks and restore the protective layer's function. The EIS test results reinforce these findings by showing that the 0.5% PAA layer has the highest impedance value and consistent phase stability after 48 hours of immersion, indicating superior corrosion resistance and self-healing ability. Thus, the HAp/PAA composite layer with an optimal composition of 0.5% PAA can be said to have the most compact, stable, and adaptive characteristics to the corrosive environment, making it highly promising as a smart and bioactive coating system for next-generation biodegradable magnesium implant applications.

ACKNOWLEDGEMENT

This work was supported by Hibah Riset UI, PUTI Pasca Sarjana Research Project, and Research Organization for Nanotechnology and Materials-National Research and Innovation Agency (BRIN) grant with the number 3/III.10/HK/2023. This work was also part of the Degree by Research Program of the National Research and Innovation Agency (BRIN).

REFERENCES

[1] N. A. Johari, J. Alias, A. Zanurin, N. S. Mohamed, N. A. Alang, and M. Z. M. Zain, "Recent progress of self-healing coatings for magnesium alloys protection," *J. Coatings Technol. Res.*, vol. 19, no. 3, pp. 757-774, 2022. DOI: 10.1007/s11998-021-00599-2.

[2] G. Cui, Z. Bi, S. Wang, J. Liu, X. Xing, Z. Li, and B. Wang, "A comprehensive review on smart anti-corrosive coatings," *Prog. Org. Coatings*, vol. 148, no. 66, p. 105821, 2020. DOI: 10.1016/j.porgcoat.2020.105821.

[3] B. Li, Z. Zhang, T. Liu, Z. Qiu, Y. Su, J. Zhang, C. Lin, and L. Wang, "Recent progress in functionalized coatings for corrosion protection of magnesium alloys: A review," *Materials (Basel).*, vol. 15, no. 11, 2022. DOI: 10.3390/ma15113912.

[4] G. S. Pereira, G. Y. Koga, J. A. Avila, I. M. Bittencourt, F. Fernandez, M. H. Miyazaki, W. J. Botta, and W. W. Bose Filho, "Corrosion resistance of WE43 Mg alloy in sodium chloride solution," *Mater. Chem. Phys.*, vol. 272, 2021. DOI: 10.1016/j.matchemphys.2021.124930.

[5] S. H. Byun, H. K. Lim, K. H. Cheon, S. M. Lee, H. E. Kim, and J. H. Lee, "Biodegradable magnesium alloy (WE43) in bone-fixation plate and screw," *J. Biomed. Mater. Res.-Part B Appl. Biomater.*, vol. 108, no. 6, pp. 2505-2512, 2020. DOI: 10.1002/jbm.b.34582.

[6] C. H. Shih, C. Y. Huang, T. H. Hsiao, and C. S. Lin, "The effect of the secondary phases on the corrosion of AZ31B and WE43-T5 Mg alloys," *Corros. Sci.*, vol. 211, p. 110920, 2023. DOI: 10.1016/j.corsci.2022.110920.

[7] V. K. Manivasagam, M. Sankar, C. B. Garcia, J. Vishnu, K. Chatterjee, S. Suwas, G. Manivasagam, and T. J. Webster, "Surface-modified WE43 magnesium alloys for reduced degradation and superior biocompatibility," *Vitr. Model.*, vol. 1, no. 3, pp. 273-288, 2022. DOI: 10.1007/s44164-022-00016-x.

[8] H. Zhang, C. Zhang, and S. D. Jiang, "Morphology evolution of hydroxyapatite: Synergistic effects and water treatment application," *Mater. Lett.*, vol. 341, p. 134288, 2023. DOI: 10.1016/j.matlet.2023.134288.

[9] S. Wen, X. Liu, J. Ding, Y. Liu, Z. Lan, Z. Zhang, and G. Chen, "Hydrothermal synthesis of hydroxyapatite coating on the surface of medical magnesium alloy and its corrosion resistance," *Prog. Nat. Sci. Mater. Int.*, vol. 31, no. 2, pp. 324-333, 2021. DOI: 10.1016/j.pnsc.2020.12.013.

[10] G. Wang, Y. Wei, J. Hong, and J. Lv, "Spray-synthesized organic composite/hydroxyapatite coating on magnesium alloys with enhanced corrosion resistance," *Front. Chem.*, vol. 13, pp. 1-11, 2025. DOI: 10.3389/fchem.2025.1566676.

[11] S. Roshan, H. E. Mohammadloo, A. A. Sarabi, and M. Afshari, "Biocompatible hybrid chitosan/hydroxyapatite coating applied on the AZ31 Mg alloy substrate : In-vitro corrosion, surface and structure studies," *Mater. Today Commun.*, vol. 30, p. 103153, 2022. DOI: 10.1016/j.mtcomm.2022.103153.

[12] H. Arkaban, M. Barani, M. R. Akbarizadeh, N. P. S. Chauhan, S. Jadoun, M. D. & Soltani, and P. Zarrintaj, "Polyacrylic acid nanoplatforms: antimicrobial, tissue engineering, and cancer theranostic applications," *Polymers*, vol. 14, no. 1259. 2022. DOI: 10.3390/polym14061259.

[13] P. Zheng, J. Deng, L. Jiang, N. Ni, X. Huang, Z. Zhao, X. Hu, X. Cen, J. Chen,

and R. Wang, "Polyacrylic acid-reinforced organic-inorganic composite bone adhesives with enhanced mechanical properties and controlled degradability," *J. Mater. Chem. B*, vol. 12, no. 34, pp. 8321–8334, 2024. DOI: 10.1039/d4tb00857j.

[14] M. E. Diken, S. Doğan, M. Doğan, and Y. Turhan, "Synthesis and characterization of poly(acrylic acid)/nanohydroxyapatite nanocomposite hydrogels and evaluation of its antibacterial, bio- and hemo-compatibility characteristics," *Int. J. Polym. Mater. Polym. Biomater.*, vol. 71, no. 18, pp. 1425-1436, 2022. DOI: 10.1080/00914037.2021.1981320.

[15] J. Yang, Y. Zhao, J. Dai, L. Han, and Q. Dong, "Surface & coatings technology fabrication and growth mechanism of multilayered hydroxyapatite/organic composite coatings on the WE43 magnesium alloy," *Surf. Coat. Technol.*, vol. 452, p. 129125, 2023. DOI: 10.1016/j.surfcoat.2022.129125.

[16] Z. Zhang, Y. Chen, D. Mandler, and M. Shenker, "Transport of hydroxyapatite nanoparticles coated with polyacrylic acid under unsaturated water flow in soil columns," *Soil Sci. Plant Nutr.*, vol. 69, no. 2, pp. 124-136, 2023. DOI: 10.1080/00380768.2022.2163457.

[17] S. Sözügeçer and N. P. Bayramgil, "Preparation and characterization of polyacrylic acid-hydroxyapatite nanocomposite by microwave-assisted synthesis method," *Heliyon*, vol. 7, no. 6, p. e07226, 2021. DOI: 10.1016/j.heliyon.2021.e07226.

[18] X. J. Ji, L. Gao, J. C. Liu, J. Wang, Q. Cheng, J. P. Li, S. Q. Li, K. Q. Zhi, R. C. Zeng, and Z. L. Wang, "Corrosion resistance and antibacterial properties of hydroxyapatite coating induced by gentamicin-loaded polymeric multilayers on magnesium alloys," *Colloids Surfaces B Biointerfaces*, vol. 179, pp. 429-436, 2019. DOI: 10.1016/j.colsurfb.2019.04.029.

[19] J. Chen, Y. Yang, I. P. Etim, L. Tan, K. Yang, R. D. K. Misra, J. Wang, and X. Su, "Recent advances on development of hydroxyapatite coating on biodegradable magnesium alloys: A review," *Materials (Basel).*, vol. 14, no. 19, pp. 1-15, 2021. DOI: 10.3390/ma14195550.

[20] K. P. P. Kumar, K. R. C. S. Raju, and R. Subasri, "Self-healing corrosion protection coatings obtained by anodization and sol–gel process on Mg AZ31 alloy," *Prot. Met. Phys. Chem. Surfaces*, vol. 58, no. 4, pp. 856-871, 2022. DOI: 10.1134/S2070205122040116.

[21] G. S. Hikku, C. Arthi, R. B. J. Robert, K. Jeyasubramanian, and R. Murugesan, "Calcium phosphate conversion technique : A versatile route to develop corrosion-resistant hydroxyapatite coating over Mg / Mg alloys based implants," *J. Magnes. Alloy.*, vol. 10, no. 7, pp. 1821-1845, 2022. DOI: 10.1016/j.jma.2022.06.005.

[22] Y. Zhao, J. Bai, F. Xue, R. Zeng, G. Wang, P. K. Chu, and C. Chu, "Smart materials in manufacturing smart self-healing coatings on biomedical magnesium alloys : A review," *Smart Mater. Manuf.*, vol. 1, no. 2, p. 100022, 2023. DOI: 10.1016/j.smmf.2023.100022.

[23] J. K. E. Tan, N. Birbilis, S. Choudhary, S. Thomas, and P. Balan, "Corrosion protection enhancement of Mg alloy WE43 by in-situ synthesis of MgFe LDH/citric acid composite coating intercalated with 8HQ," *Corros. Sci.*, vol. 205, p. 110444, 2022. DOI: 10.1016/j.corsci.2022.110444.

[24] M. Ostapiuk, J. Bieniaś, M. V. Loureiro, and A. C. Marques, "The effect of self-healing on the corrosion resistance of a Mg alloy promoted by isocyanate microcapsules of polyurethane/polyurea shell," *J. Mater. Eng. Perform.*, vol. 6, 2025. DOI: 10.1007/s11665-025-11760-y.

[25] A. S. Gnedenkov, V. S. Filonina, S. L. Sinebryukhov, and S. V. Gnedenkov, "A superior corrosion protection of Mg alloy via smart nontoxic hybrid inhibitor-containing coatings," *Molecules*, vol. 28, no. 6, 2023. DOI: 10.3390/molecules28062538.

[26] N. S. Grewal, U. Batra, K. Kumar, and A. Mahapatro, "Novel PA encapsulated PCL hybrid coating for corrosion inhibition of biodegradable Mg alloys: A triple-triggered self-healing response for synergistic multiple protection," *J. Magnes. Alloy.*, vol. 11, no. 4, pp. 1440-1460, 2023. DOI: 10.1016/j.jma.2023.01.019.

[27] Z. Shi, F. Yang, Y. Hu, Q. Pang, L. Shi, T. Du, Y. Cao, B. Song, X. Yu, Z. Cao, Z.

Ye, C. Liu, R. Yu, X. Chen, Y. Zhu, and Q. Pang, "An oxidized dextran-composite self-healing coated magnesium scaffold reduces apoptosis to induce bone regeneration," *Carbohydr. Polym.*, vol. 327, p. 121666, 2024. DOI: 10.1016/j.carbpol.2023.121666.